ISSN 1063-7397, Russian Microelectronics, 2014, Vol. 43, No. 6, pp. 377–387. © Pleiades Publishing, Ltd., 2014.
Original Russian Text © A.V. Tsukanov, I.Yu. Kateev, 2014, published in Mikroelektronika, 2014, Vol. 43, No. 6, pp. 403–414.

Quantum Calculations on Quantum Dots in Semiconductor Microcavities. Part II

A. V. Tsukanov and I. Yu. Kateev

Institute of Physics and Technology, Russian Academy of Sciences, Nakhimovskii pr. 34, Moscow, 117218 Russia
e-mail: tsukanov@ftian.ru, ikateyev@mail.ru

Received April 8, 2014

Abstract—In this work we continue considering solid hybrid systems formed from semiconductor quantum dots and microcavities integrated into a single optical scheme. In the second part, the main emphasis is on the methods of investigation and on the schemes for recording of the spectra and the time dependences of the population energy level, which illustrate the modern control level of the quantum state of these systems.

DOI: 10.1134/S1063739714060092

1. INTRODUCTION

Theoretical analysis of the properties of the systems based on quantum dots (QDs) coupled to microcavities (MCs) suggest the emergence of specific features in the spectra of each subsystem accounting for their hybridization (see first part of the review [1]). The second part of our review will be devoted to the methods of the experimental investigation of the spectra and of the dynamics of solid nanosystems of the QD + MC type. In addition to the approaches well known in quantum optics, such as recording of photoluminescence and monitoring of the QD population in time, we will introduce basic principles of reflectometry and transmission measurements suggested relatively recently that provide the possibility of testing optical properties of these objects at a single photon level. The main results of the experiments obtained within the last few years will be presented.

2. EXPERIMENTAL METHODS FOR INVESTIGATION OF QD PROPERTIES IN CAVITIES

As we have seen (see part I [1]), the description of the QD dynamics with the help of equations (10)–(13) is based on the knowledge of phenomenological values (coupling constants and dissipation rates) that appeared in them. The calculation of these values within one microscopic model or another requires, in turn, consideration of the exciton (electron) density distribution in the QD states, coordinate dependence of the MC mode fields, QD localization in MCs, and relative orientation of their symmetry axis, which is a rather complicated procedure. Unique experimental techniques were developed as an alternative for the determination of optical parameters of solid-state optical quantum systems. Recording photoluminescence (PL) spectra remains one of the most widely used methods for investigation of hybrid systems in the mode of both strong and weak QD coupling to MC. Peaks are observed in the PL spectrum of the sample under off-resonance conditions that correspond to the frequencies of the MC intrisic modes and transition frequencies in the OD. It is interesting that the photons emitted from QDs as a result of recombination of exitons generated by the external electromagnetic field serve as a source of PL for both of the subsystems. These peaks start coming closer together under condition of tuning the QDs in resonance with the MCs via any of the methods described in part I (section 2). They overlap under condition of weak coupling generating one single maximum for the QDs and the cavity. The double peak (Rabi splitting) is observed under conditions of strong coupling when the QD and MC frequencies coincide. In general, the scheme for the PL spectra recording is the following. The system is placed into a helium cryostat and cooled to a temperature of 4.2–50 K. Electron-hole pairs in the QDs are excited by a laser with fixed or tunable wavelength λ_L. The laser beam is focused on a sample surface directly above the QDs by the confocal microscope objective with aperture ranging from 0.4 to 0.75; the size of light spot comprises few microns in the process. The recombination photons emitted from the system with the wavelength λ_{em} are collected by the same objective, forwarded to a spectrometer, and detected by a CCD camera. Time-resolved spectroscopy is used for determination of the spontaneous photon emission rate. In this case the sample is irradiated by a pulsed laser, and the photon detection is carried out by an avalanche photodiode [2, 3] or superconducting single photon detector [4].

Which data on the optical system can be generated from the analysis of PL spectra? Firstly, the information on the mode, in which the QDs and MCs exist, is of practical interest from the point of view of the QD

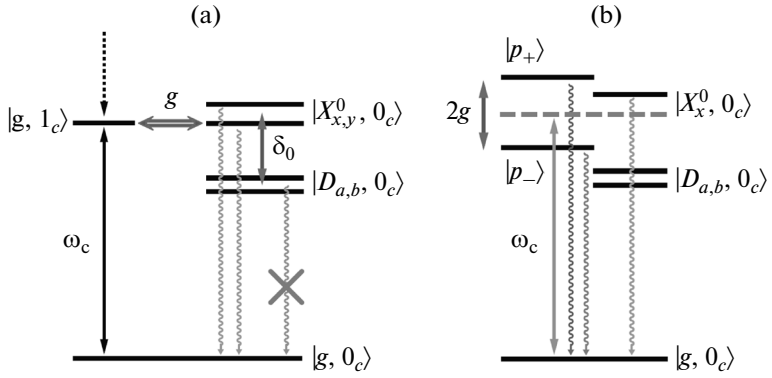

Fig. 1. Scheme of optical transitions between the ground state and the states of one-exciton multiplet of a single quantum dot (a). One of the multiplet states $\left|X_y^0,0\right\rangle$ can exchange photon with MCs with the Rabi frequency g. Scheme of optical transitions between the vacuum state of a hybrid QD + MC system, polariton states $|p_\pm\rangle$, and $\left|X_x^0,0\right\rangle$ state (b). The MC modes are coupled only to the $\left|X_y^0,0\right\rangle$ state of the QDs [5].

application as functional elements in high technology devices. As mentioned above, the answer to this question can be obtained from the investigation of the spectrum structure in the vicinity of the QD and MC frequency resonance: singlet (doublet) indicated the mode of weak (strong) coupling. This predetermines the ways of further application of the system. On the other hand, it is not always possible to determine which of the OD optical transitions contributes to the PL spectrum. The procedure of spectral line assignment of the single QD (InAs) in the L3-cavity (Q = 16000 for λ_c = 931.5 nm) at T = 4.2 K was demonstrated by the authors in [5]. Considering that the QD one-exciton state comprises an electron-hole pair, in which the electron spin projection is ±1/2 and the hole pseudo-spin is ±3/2, the projection of the total angular moment can assume only four values, $M = \pm1, \pm2$. The intrinsic vectors $\left|D_{a,b}\right\rangle = \left(\left|+2\right\rangle \pm \left|-2\right\rangle\right)/\sqrt{2}$ formed from the linear combination of magnetic states with $M = \pm2$ represent "dark" states because the radiative recombination of such excitons accompanied by the QD transition into a vacuum state is forbidden by the selection rules, according to which the angular moment projection can change by the value $\Delta M = \pm1$. The states $\left|X_{x,y}^0\right\rangle = \left(\left|+1\right\rangle \pm \left|-1\right\rangle\right)/\sqrt{2}$, on the other hand, are bright states, which decay with the emission of a single photon. The hole and electron spin exchange interaction results in the $\delta_0 \sim$ 100–200 μeV splitting of the dark and bright doublets, as well as the interdoublet splitting <30 μeV (see Fig. 1a). Moreover, the MC geometric parameters were selected in such a way that the electric field of its fundamental mode is directed along the y axis perpendicular to the L3-defect axis. Hence, only the $\left|X_y^0,0\right\rangle$ state (1 y exciton in the QDs and 0 photons in the MCs) could effectively interact with the state $\left|0,1\right\rangle$ (0 excitons in the QDs and 1 photon in the MCs) via the quantum exchange, while the $\left|X_x^0,0\right\rangle$ state would be isolated from the MC mode. This interaction, as we know, results in formation of the Jaynes-Cammings polariton doublet, $\left|p_\pm\right\rangle = \left(\left|X_y^0,0\right\rangle \pm \left|0,1\right\rangle\right)/\sqrt{2}$, as is shown in Fig. 1b. The authors in [5] excited the transitions in the system with the help of a laser pump (λ_L = 818 nm, P = 10 nW) and analyzed the PL with a 30 μeV-resolution spectrophotometer. The MC wavelength was scanned in the range from 931.5 to 936 nm due to deposition of the gas molecules onto the semiconductor surface (see part I). The PL intensity is the function of wavelengths λ_c and λ_{em}. It is easy to see that the emission spectrum demonstrates several anticrossings assigned by the authors to the states X^+ (1 exciton and 1 hole), X^0 (neutral exciton), and XX^0 (neutral biexciton) in the order of increasing λ_{em}. The highest splitting value (316 μeV) is observed for the polariton doublet state $\left|p_\pm\right\rangle$ in the group of the lines X^0, while for the X^+ states, this value is 205 μeV. The authors found the X_x^0 singlet line by conducting additional data processing, as well as the X^{1-} and X^{2-} lines corresponding to the single- and double-negatively charged excitons (trions). They were able to prove the effect of superfine QD exciton interaction with nuclear spins of the crystalline lattice resulting in the hybridization of the dark and bright doublets.

In the majority of studies the QD laser pumping is conducted under off-resonance conditions. The electron-hole pairs in this case are formed in the wetting layer of the heterostructure due to the absorption of photons with energy exceeding the energy of the exciton in the QDs. Next, they lose their energy due to the scattering on the crystalline lattice phonons, are captured by the QDs and, finally, recombine with the

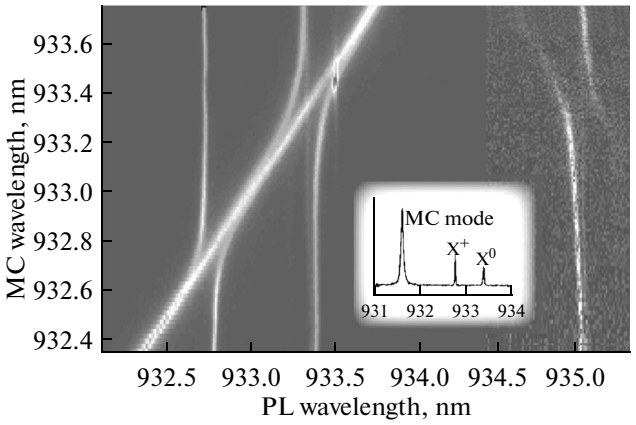

Fig. 2. Dependence of the PL intensity on the MC mode wavelength and wavelength of photons emitted from the structure demonstrating anticrossings for X^+ and X^0 and biexciton transitions (from left to right). The PL spectrum for the case when the MC mode was detuned to the blue frequency region relative to the QDs [5] is presented in the inset.

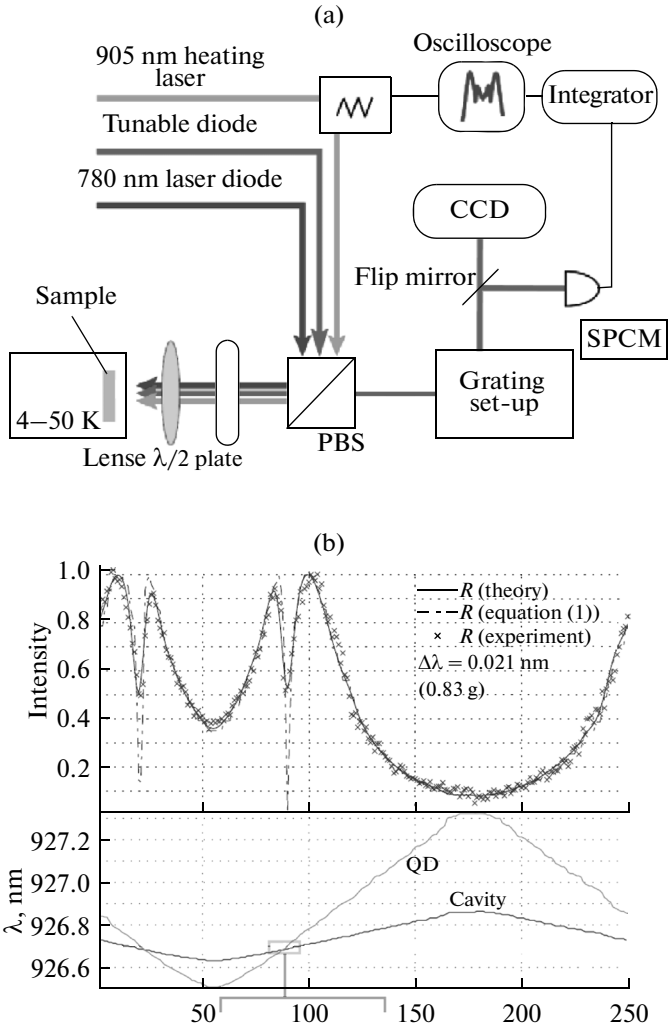

Fig. 3. Scheme of optical setup for measuring PL spectra and reflection coefficient from a QD + MC system (see text): (a) intensity of the reflected probing signal (top) with frequency detuned from the QD frequency by $\Delta\lambda$ as a function of the QD and MC frequency detuning (bottom) and effective temperature (abscissa axis); (b) symbols, experiment; solid line, modeling; dotted-and-dashed line, Eq. (1) [7].

emission of the PL quantum. This method of the optical transition excitation displays a number of drawbacks (see below) and cannot be used for the targeted coherent action on the QDs. The improvement of the technique demonstrated in [6] includes the use of the resonance QD (MC) pumping by the pulsed laser followed by recording of the MC (QD) emission. Despite the detuning of the subsystem frequencies, the excitation energy is distributed between them due to the effects of dissipation. This approach proves the possibility for measuring the QD spectrum with very high resolution.

Following the spectral lines' assignment, the QD and MC parameters can be determined. Let us briefly list the main methods allowing us to determine all the parameters that characterize a hybrid system. The rate of photon dissipation in MCs (or Q factor) κ is determined under conditions of intensive irradiation by the external laser transferring the QDs into the saturation mode, due to which the main contribution into the spectral line broadening is provided exclusively by the process of photon dissipation. The rate of the QD relaxation γ is determined as a decrement of the decline of the time dependence of its excited state population under condition of detuning $\delta_{a,c}$ of the QD and MC frequencies. The rate of the QD dephasing γ_d is found via interferometric analysis of the PL signal in the Hong-Ou-Mandel system. The coupling coefficient g of the QDs with MCs can be calculated using the equations given in the section 3 of part I, provided all these parameters are known and the detuning is fixed close to the resonance.

The group from Stanford University (California, USA) led by J. Vuckovic was very successful in the investigation of hybrid systems. This group of American scientists created a universal optical setup (Fig. 3a), with the help of which it is possible to test the optical response of nanostructures under different excitation modes [7]. A continuous diode laser with a frequency slightly above the frequency of the interzone exciton transition and power of 20 nW is used in this setup for recording the frequency spectrum via direct measurement of the PL intensity. The frequency of the MC mode is scanned in the vicinity of the QD transition by varying the sample temperature in the range from 27 to 33 K using a heating titanium-sapphire laser (905 nm) in the power range from 6 to 300 μW. The single exciton line of the QD spectrum is split into a polariton doublet at the resonance frequencies. The following parameters are determined from the obtained dependences using fitting algorithms: (a) broadening of the

MC mode (rate of photon dissipation), $\kappa/2\pi = 16$ GHz, (b) broadening of the QD line (rate of direct relaxation), and the $\gamma/2\pi = 0.1$ GHz, (c) coupling coefficient of the cavity mode to the QDs (Rabi frequency) $g/2\pi = 8$ GHz [7], (d) rate of the dephasing $\gamma_d/2\pi = 3$ GHz, and (e) rate of the combined photon-phonon relaxation $\gamma_r/2\pi = 0.5$ GHz (at $\delta_{a,c} = 8\kappa$) [8]. A low-power ($P_{in} = 3$ nW) probing diode laser is used for more accurate determination of these parameters with the help of the analysis of the reflected signal intensity (reflectometry). The laser detuning from the point of anticrossing is comparable with the anticrossing value ($\Delta\lambda \approx 0.05$ nm) in the process, and the average number of quanta $\langle n_c \rangle \approx \eta P_{in}/2\kappa\omega_c$ injected into the system does not exceed 0.003. It must be noted that considering the fact that the efficiency of the laser interaction with the system was extremely low ($\eta \approx 1$–2%), the authors increased the detector resolution by using a polarization filter. The laser photons with vertical polarization $|V\rangle = |V + H\rangle + |V - H\rangle$ hit the semiconductor surface at an angle of 45 degrees. Hence, the reflected component takes the form $-t(\omega)|V + H\rangle - |V - H\rangle$, where $t(\omega)$ is the reflection amplitude. The beam splitter transmits only horizontally polarized photons in the detection direction and, consequently, the intensity of the measured signal is proportional to $|1 - t^2(\omega)|$, which provides the possibility to determine the reflection coefficient R.

Analytical expression

$$R = \eta \left| \frac{\kappa}{i(\omega_c - \omega) + \kappa + g^2 / [i(\omega_a - \omega) + \gamma]} \right|^2 \quad (1)$$

allows calculating phenomenological constants via fitting. A typical graph of the intensity versus detuning $\delta_{a,c}$ is presented in Fig. 3b. The slight discrepancies between the experimental and theoretical values determined by this method are explained by the stochastic fluctuations ($\delta\lambda \sim 0.005$ nm) of the system frequencies that occur due to the instability of the heating laser power ($\delta P_L/P_L \sim 0.7\%$). The radiation emitted or reflected by the system is focused by the system of lenses, analyzed by monochromator (diffraction grating), and followed by the measuring of the intensity by the light-sensitive element at the temperature of liquid nitrogen. The results of the experiments indicate good agreement between both types of data.

Note that the reflectometry is considered to be a more sensitive method than the PL spectra measurement, allowing us to conduct quantum monitoring of the system at a single photon level. The authors of [7] and [9] focus their attention on the fact that this approach provides the possibility to improve the measurement accuracy, which is determined in the case of PL analysis by the spectrometer resolution of ~0.03 nm, to the value of <0.005 nm, which is determined by the detector measuring the wavelength of the reflected photon. Another significant advantage of the reflectance measurements is that it provides the possibility of the MC testing without the QDs, as the availability of the secondary emission is not required in this case. The spectrum of the signal reflected from the "empty" MCs can be calculated from Eq. (1), assuming $g = 0$. The theoretical results are in quantitative agreement with the experimental data, with minor differences emerging due to the technological defects [9]. The additional modification of the reflectometric scheme [10] allows increasing the signal/noise ratio to 900 (instead of 100 for the standard reflectometer) by using the differential spectroscopy technology, as well as monitoring the response of the MC mode with random polarization using the homodyne detection technique.

Transmission spectroscopy comprising the measurement not of the laser probing pulse reflected by the system but the transmitted one represents a method for investigation of hybrid structures that is close to reflectometry [11]. The typical scheme of a setup including a waveguide additionally to the QDs and MCs is presented in Fig. 4. A vertical incident photon beam interacts with the MC mode that is coupled weakly to the QDs and next the photons absorbed by the system arrive to the waveguide due to the dissipative contact of the MCs and waveguide (extended linear defect PC). One of the waveguide ends is equipped with a diffraction grating comprising a semicircle with the radius equal to the waveguide mode, which is separated in the middle by a semi-ring with the thickness of $\lambda/2n$ (n is refractive index of the material). This grating design allows blocking the propagation of the light wave leaving the waveguide in the horizontal plane and reorienting it vertically in the direction of the detector. The spatial filter (pinhole) must be used in this case in front of the confocal microscope objective that transmits only photons scattered by the grating. The dependence of the photon transmission coefficient of the system on their frequency is as follows (compare with Eq. (1)):

$$T = \left| \frac{2\sqrt{\eta_{wg}\eta_a}\kappa}{i(\omega_c - \omega) + \kappa + g^2 / [i(\omega_a - \omega) + \gamma]} \right|^2, \quad (2)$$

where coefficients η_{wg} (η_a) characterize the efficiency of the MC mode coupling to the waveguide (photon source). The authors [11] showed that the ratio of the intensity of the signal collected with the help of grating

and the signal arriving from the MCs was 0.64. All advantages of the reflectometry scheme are retained in this method; and the device presented in Fig. 4 represents a valid element of the quantum network. The authors also discuss the integral design of the quantum chip consisting of several such elements with independent control and common waveguide, which combines them all via photon tunneling, performing both measuring and transport functions.

It is possible to use a near-field scanning optical microscope in order to confirm the presence or the absence of the QD coupling to the MC mode, as well as to obtain the quantitative view on the spatial dependence of the intrinsic MC mode field strength. Optical fiber serves as a major element of this device, through which the control laser pulse irradiates the sample surface and the emission is guided to the spectrometer. Moreover, bringing the optic fiber end 5–10 nm closer to the surface results in the noticeable modification of the medium dielectric constant and, consequently, in the change of the refractive index of the cavity material and of its intrinsic mode frequencies. This provides the possibility to assign the spectral peaks to one subsystem or another. The 0.14 nm-shift of the wavelength of one of the H1 defect mode of the PC was demonstrated in [12], which was due to the vertical movement of optic fiber, while the positions of the exciton and biexciton transition spectral lines in the QDs located in the central region of the defect at the depth of 160 nm from the surface remained unchanged. If the subsystem frequencies vary significantly, the QD position in the substrate can be identified or the field profile of the mode on the surface can be obtained by monitoring the coordinate dependence of the emission from the QDs or the mode frequency. If the subsystem frequencies are close, a conclusion on the nature of their coupling can be made based on detection of the changes in the intensity and resonance frequencies.

In addition to the methods based on the PL measurements of the PC defects with QDs under the action of laser fields, it is possible to investigate their optical properties, as well as the processes of capture, relaxation, tunneling, and recombination of the carriers in the QDs via monitoring of the electroluminescence (EL) spectra. To do this the investigated sample must be incorporated into a photodiode structure consisting of semiconductor layers doped with electrons (*n*-layers) and holes (*p*-layers) in such a way that the voltage applied to the *p*- and *n*-layers will be along the axis of the heterostructure growth. The qualitative agreement between the PL and EL spectra was observed in [13]. The authors investigated various regimes of the QD excitation: off-resonant with wavelength 633 nm, quasi-resonant (971 nm), and resonant (1060 nm). The electron-hole pair energy is found to be higher than the forbidden zone width in the case of the off-resonant regime, and, hence, the carriers leave the QDs easily. The pair energy corresponds to one of the states close to the QD edge under the quasi-resonant excitation, also providing the possibility for the electron tunneling from the QDs. The pair energy is close to the energy localized on the QD *p*-orbital in the case of resonant excitation and, hence, the process of exciton recombination is the most probable. The PL peak intensity decreases with the increase of the applied voltage in the case of off-resonant and quasi-resonant regimes, with the PL suppression by the electric field occurring more effectively in the off-resonant regime, than in the quasi-resonant one. Competition exists between the processes of exciton recombination, resonance tunneling of the carriers from QDs, and their relaxation at different regimes of the QD excitation.

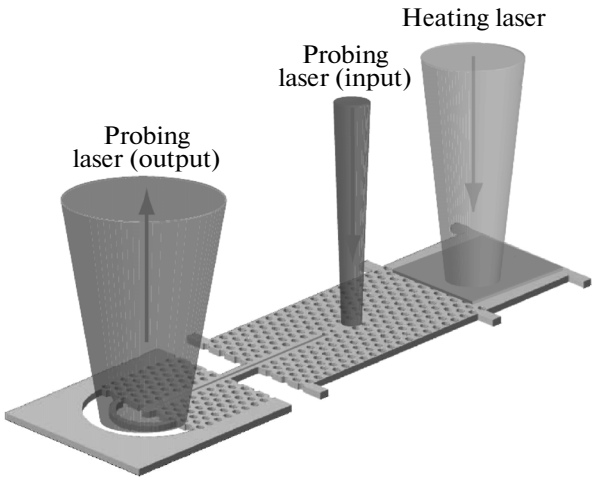

Fig. 4. Principle of transmission spectroscopy used for measuring the state of the QD + MC hybrid system. Heating laser controls detuning of subsystem frequencies. The probing laser photons interact with the system and are withdrawn through the one-dimensional waveguide integrated in the system to the output equipped with grating. The flux of photons scattered from the system is directed to the detector [11].

In addition to the thermal and electromagnetic noise, a series of significant drawbacks characteristic of the spectroscopic methods for the investigation of hybrid systems exists. For example, the same parameters determined by different alternative techniques—by the PL spectra analysis and by analysis of the time dependences of the QD excited state population—can differ considerably. The following sources of errors are mentioned: (a) the availability of multiexciton complexes in the given QDs and excitons in the neighboring QDs that transform the emission from a single QD into a collective one, and (b) interference of the electromagnetic fields emitted from the QDs and MCs on the detector. The first issue results in the several-fold overestimation of the coupling coefficient *g*, which interferes with the correct identification of the subsystem coupling regime, and the second one results in the incorrect determination of the partial PL intensi-

ties from the QDs and MCs. The temporal measurements provide more accurate results than the spectroscopic observations as is shown in [14]. They are in good agreement with the theoretical predictions. It is related to the fact that the instrumentation used for temporal measurements tuned to the analysis of a small part of the spectrum in the vicinity of the given QD frequency allows decreasing the effect of other QDs. Moreover, the processing of the graphs of population time dependences allows for all the multiexciton contributions to be excluded and the decline in the decrement related to the single-exciton QD relaxation to be determined.

Statistical analysis of photon correlations plays an important role in the investigation of the optical properties of the hybrid structures. Usually it comprises construction of an experimental graph of the second order autocorrelation function $g^{(2)}(\tau)$ versus the delay time τ of the detection of two consecutive photons emitted from the system and, in particular, determination of the $g^{(2)}(0)$ value [15, 16]. When this value is below 0.5, the system emits in a single-photon regime characterized by the photon antibunching. This type of statistics is observed under conditions of photon blockade, when the laser pulse resonantly tuned to the system transition from the vacuum to the polariton state of the first Jaynes–Cammings doublet injects only a single quantum of the respective frequency into the system. When the laser frequency equals the MC frequency, the resonance with the polaritons of the second doublet takes place, at which the probability of simultaneous absorption and following emission of two photons is high ($g^{(2)}(0) > 1$), corresponding to their bunching. We note that this type of experiment, in which the nonlinearity of the hybrid system spectrum and sub-Poisson statistics of the secondary radiation are manifested clearly, provide strong evidence of the quantum nature of the field and matter interaction. We will return to the analysis of the statistical properties of photons emitted from the hybrid QD systems in section 4 during the discussion of their potential use as single-photon sources.

Below we present the results of most prominent studies devoted to the experimental investigation of the QD and MC coupling obtained with the use of methods described in this section.

3. RESULTS OF EXPERIMENTAL INVESTIGATIONS OF COUPLED QD AND MC

As mentioned above, modification of the spectra and relaxation times of the hybrid QD systems by the MC photon field represented its important property. Two quantitative parameters exist that are used for estimating the degree of interrelation between these subsystems. One of them—*Purcell factor F* (see equation (9) in part I)—characterizes the change of the emission rate of the excited QDs due to its contact with the MC mode. Another parameter—β-*factor*—equals the percentage ratio of the photon emission rate from the QD into the MC optical mode to the rate of total emission. Both these parameters were determined in [17] for the system consisting of several QDs located in the waveguide channel. The PC comprised a 150 nm thick GaAs-membrane with a lattice constant of 256 nm and hole diameter of 76.8 nm, and the waveguide of 100 μm length was formed from a region without holes. Five narrow peaks from different QDs and a wide maximum from the allowed waveguide zone were clearly visible in the PL spectrum of the sample recorded at 10 K. The emission rate from the isolated QDs determined by monitoring the decline of its excited state population was 1.1 ns^{-1}. The measurements showed that the photon emission rate increased to 5.7 ns^{-1} with the closing of the gap between the frequency of one of the QDs and the waveguide frequency, while it decreased to 0.8 ns^{-1} with the increase of the detuning from the resonance. The Purcell factor, $F = 5.2$, and the β-factor equaling 85% for this system were calculated based on these measurement data. The results of similar measurements conducted for the remaining four QDs showed that the β-factor was in the range 63–85% at the resonant tuning with the waveguide mode.

The emission spectra of three MC—PC defects with *Q*-factors of 200, 250, and 1600 containing QDs—were investigated in [18]. The maxima around the 900 nm wavelength corresponding to the MC modes were observed in the PL spectra (Fig. 5a). One of the exciton peaks of the QD spectrum (exciton line *A*) was located close to the MC mode for all the samples, and the sharp decrease of the photon lifetime τ was observed for it. It decreased from $\tau_0 = 1.7 \pm 0.3$ ns (QDs outside the cavity) to $\tau_A = 650$ ps for one of the tested samples. Hence, the rate of spontaneous emission increased 2.6 ± 0.5-fold. In contrast, the lifetime of photons of the same wavelength but orthogonal polarization and, consequently, located out of resonance with the defect mode increased to 2.9 ns in the process. The increase of the photon lifetime was observed also for the other exciton states (lines *B* and *C*) with the wavelengths differing significantly from the wavelength of the PC defect mode, Fig. 5b. Similar results were obtained for all the samples. Corrective tuning of the exciton line *A* into resonance with the MC dipole mode carried out by changing the sample temperature enhanced the Purcell effect (the τ_A value decreased to 210 ps, and the rate of spontaneous emission increased 8-fold). The decrease (increase) of the spontaneous emission rate for all the cases when the QD exciton transition was in the PC's forbidden zone (close to the frequency of the optical mode of the L3 defect) was also demonstrated in [3]. The temporal measurements showed that when the photon lifetime in the QDs outside of the PC was 0.66 ns, it increased to 13.1 ns in the case when the QD frequency was in the PC's forbidden zone. In contrast, when the QD

and the MC mode frequencies were brought together, this was accompanied by the decrease of the photon lifetime from 750 ps to 90 ps, which allowed estimating the Purcell factor as $F \sim 8$.

Due to the Purcell effect, the MCs can not only enhance the emission radiation at frequencies close to the intrinsic frequencies of the defect modes but also change its polarization. This effect was experimentally proven in [19], where the emission from a single QD weakly coupled to a MC was investigated. Initially the polarization vector of the major part of the photons emitted from the QDs was orthogonal to the polarization vector of one of the PC defect modes. The shift of the QD peak toward the maximum of this mode was observed in the PL spectrum with the sample heating. The polarization vector of the recorded photons changed in the process and, finally, the majority of them had polarization coinciding with the polarization of the optical mode. The reason for the change in the emission polarization vector is related to the emission enhancement of only those photons with polarization close to the polarization of the cavity mode.

A unique method for controlling the photon spontaneous emission rate was suggested in [20]. Considering that according to Eq. (9) the F value depends on the Q-factor, the F can be changed via changing the Q value. The sample comprised optical interface consisting of two PCs (left and right), which have different lattice parameters (Fig. 6). The L3 type defect cavity was in the *left* PC, and the waveguide was located at a certain distance from it that comprised an extended linear defect formed by the region in the PC lattice lacking the holes. Considering that the frequency of the intrinsic MC mode corresponded to the forbidden zone of the spectrum of the *right* PC, the photons leaving the MCs and propagating along the waveguide to the right were reflected and interfered with the photons propagating to the left. When the interference was destructive, the decrease of the number of photons leaving the left end of the waveguide was observed and, consequently, the Q-factor of the optical system increased. The interference nature was preset by the local change of the waveguide refractive index.

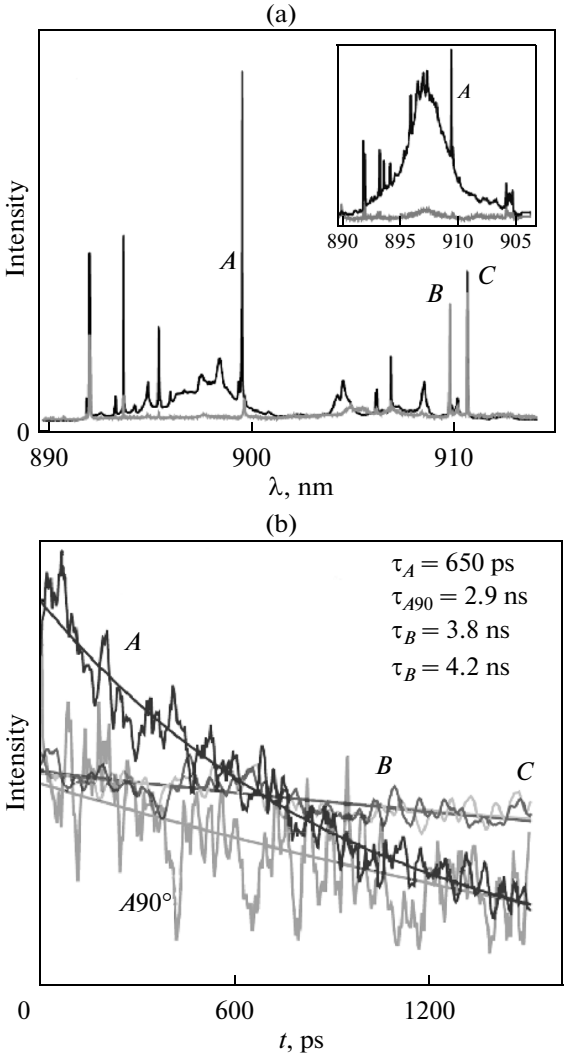

Fig. 5. PL spectrum of the GaAs cavity with QDs: (a) the spectrum peaks correspond to exciton lines *A*, *B*, and *C* at the weak coupling mode; inset: PL spectrum at high intensity pumping. Results of measurement of photon lifetimes and (b) for exciton lines *A*, *B*, and *C*. *A*90° denotes exciton line *A* with polarization of photons emitted from QDs perpendicular to the MC polarization mode [18].

It was already mentioned that the resonant laser pumping of the QDs was found to be more effective than the off-resonant. The same situation takes place in relation to the QD pumping via MCs using a laser with the wavelength that does not coincide with the wavelength of one of the MC modes. It can be suggested that the laser frequency tuning in resonance with the MC mode (MC defect mode for example) could significantly improve the efficiency of the QD pumping. This effect was demonstrated in [21], where the effect of the pump laser wavelength on the photoluminescence spectrum of the PC-cavity was investigated. The peaks corresponding to the MC defect modes, the first of which had wavelength $\lambda_0 = 1060$ nm, were observed in the PL spectrum recorded after the off-resonance action of helium-neon laser with the fixed wavelength. The wavelengths of $\lambda_1 = 1000$ nm and $\lambda_2 = 947$ nm corresponded to the modes of higher order. Next the PL spectrum as a function of λ was produced using the continuously tunable titanium-sapphire laser. It was found that when the λ coincided with λ_2, the PL spectrum demonstrated the peak at the wavelength λ_0. The peak intensity was found to be one order of magnitude lower in the off-resonant case ($\lambda \neq \lambda_2$), when the pump photon wavelength λ was 945 nm. This is related to the fact that the MCs effectively absorbed photons with the wavelength of one of its intrinsic modes at $\lambda = \lambda_2$, which, in turn, excited the QDs. The QDs emitted light in a wide range on the transition to the ground state, and the MCs enhanced the emission

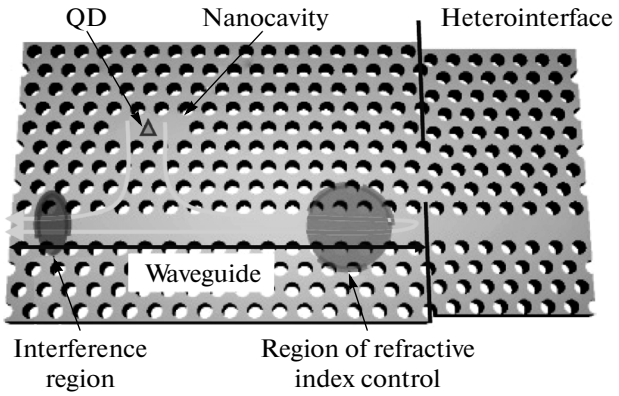

Fig. 6. Schematic representation of optical interface consisting of two GaAs PC with different lattice parameters. The InAs QD is located in the left PC. Q-factor is controlled with the local change of the waveguide refractive index (shaded area on the right) [20].

of photons with the wavelength λ_0 of its fundamental mode due to the Purcell effect.

As we know, one of the criteria for the attainment of strong coupling in hybrid systems is the splitting of the single peak in the subsystem spectrum (Rabi splitting), when their frequencies are close to each other. The QD and MC peak intensities, as well as their widths, become practically the same in the process. Strong coupling is observed in the PC with different types of defects, with the L3-type defect being the most common in the experiments [22, 23]. The Rabi splitting in the PC with an H1-type defect in the MCs was also observed in [23]. Considering that the volume V of the fundamental doubly degenerated dipole mode of such defects is found to be half of that for the L3-type MC, it can be suggested that the coupling coefficient g, which is in inverse proportion to $\sqrt{V}$, will be higher. Following the temperature resonance tuning of the QD and MC frequencies the Rabi splitting was observed, which was approximately 124 μeV corresponding to the value $g = 76$ μeV. Both peaks demonstrated the same width of 0.082 nm (the peak width of the single QD was 0.03 nm, and the peak width of the cavity was 0.14 nm). An alternative technique of the electric tuning of the QD spectrum through the Stark effect allowed demonstrating the regimes of weak and strong coupling between the QDs and high Q-factor MCs ($Q \sim 12\,500$) [24]. We again note that the spectroscopic measurements of the Rabi frequency require caution and analysis of all the recombination processes in order to decrease the experimental error resulting in the overestimation of the g value.

It must be mentioned that in the majority of the considered studies the QD + MC systems do not have an input/output interface (excluding the systems designed specifically for transmission measurements). A reliable and effective way for the transfer of quantum information between the system nodes must be designed in order to create a functional quantum network based on them. The well-known PC-waveguides can be used as interaction mediators of the separated QD-qubits. A strong coupling of the waveguide (extended linear defect of PC) and the single QD was observed in [25]. The defect cavity containing the QDs was formed by the lattice holes shifted relative to the waveguide. The suggested configuration of the device allows transporting the QD quantum state encoded in the photon state along the waveguide. The QD exciton spectrum was resonantly tuned to the waveguide mode using the temperature change. The Rabi splitting was 140 μeV under condition of strict resonance, and the coupling coefficient of the QDs and waveguide was estimated as $g \sim 82$ μeV.

4. SINGLE PHOTON SOURCES BASED ON QDs AND MCs

The semiconductor QDs embeded into optical networks are promising candidates as single photon sources for application in various areas, in particular, quantum informatics and metrology [26–28]. Theoretical [29, 30] and experimental [31–34] studies of the properties of such quantum sources have been conducted for a long time. As mentioned above, the construction of the second order autocorrelation function $g^{(2)}(\tau)$ that described the correlation of the electromagnetic field intensity I of the two sequentially detected photons,

$$g^{(2)}(\tau) = \frac{\langle I(t)I(t+\tau)\rangle}{\langle I(t)\rangle^2}, \qquad (3)$$

represented one of the popular methods for investigation of the photon statistics. The $g^{(2)}(\tau) = 1$ for the classical sources with chaotic light emission such as the laser or light emitting diode, which indicates the lack of any correlation between the two photons. Considering that the quantum source emits one photon (or a pair of entangled photons) for each excitation pulse, the measurement of the autocorrelation function at zero delay time gives $g^{(2)}(0) < 1/2$. In the case of an ideal single photon source, $g^{(2)}(0) = 0$, because the source cannot generate more than one photon within the excitation period.

Due to the Purcell effect, it is possible to increase the spontaneous photon emission rate emitted on the exciton recombination via the introduction of QDs into a high quality cavity. One of the methods to achieve high efficiency of the single photon sources based on hybrid systems is the selection of MCs. For example, the PC structure with the optimized hole radius and enlarged lattice constant was fabricated in [31] for investigating the single photon generation. The excitation laser pulse was focused on the surface of a two-dimensional PC in the defect region containing a single QD, and the photon withdrawal was car-

ried out with 24% efficiency through the waveguide formed in the same PC structure. It is possible to improve the source quality via the QD resonant excitation through one of the intrinsic MC modes. It was shown in [33] that at the laser power of 1 μW the intensity of the PL exciton peak at the resonant pumping was 25-fold higher than at the pumping through the wetting layer. According to the autocorrelation function measurements, single photon generation was observed in both cases; however, the laser power was 100-fold lower in the case of the resonant excitation as compared with the off-resonant one, and the photon was emitted only from the QDs located in the node of the MC mode, while the emission from the rest of the QDs was suppressed.

Since the frequency of the single photons emitted by the source based on QDs is close to the frequency of the exciton transition (~1 μm) it is important from the practical point of view to transform it. The method for the frequency increase demonstrated in [32] involved the following procedure: the 1300-nm photons emitted from the InAs QDs on the pulse laser pumping with a wavelength of 780 nm and the repetition frequency of 50 MHz propagated through the $LiNbO_3$ waveguide with a one-dimensional periodic structure (Fig. 7). The controlled time profile pulses of light with a wavelength of 1550 nm and repetition frequency of 25 MHz preset by the electric modulation of the laser radiation were delivered to the waveguide. The single photons at the waveguide output had a wavelength of 710 nm, which corresponded to the sum of the QDs and modulator frequencies, and the shape of its time profile changed from the exponential decay characteristic for the QD radiation to the Gaussian.

One of the most important properties of the single photon source is the *indistinguishability* of the two sequentially emitted photons, which must have the same frequency, polarization, and time profile. In the real experiments, the photons become distinguishable due to their interaction with the environment that destroys coherence. The degree of the photon indistinguishability measured with the use of the Hong–Ou–Mandell interferometer is determined by the value [34, 35]

$$W = \frac{\gamma}{2\gamma_1} \approx 1 - g^{(2)}(0), \qquad (4)$$

where $\gamma_1 = \gamma + \gamma_d/2$, γ is the rate of energy dissipation from the quantum emitter and γ_d is the rate of its dephasing. Despite the fact that it is very difficult to suppress the dephasing process, its effect can be reduced by increasing the γ. When the QD is a quantum emitter, there is a possibility due to the Purcell effect to significantly accelerate the photon emission via the QD formation inside the MC. For example, the use of the GaAs PC-cavity with the H1-type defect and a Q-factor of approximately 250 allowed the authors in [34] to reach the indistinguishability degree

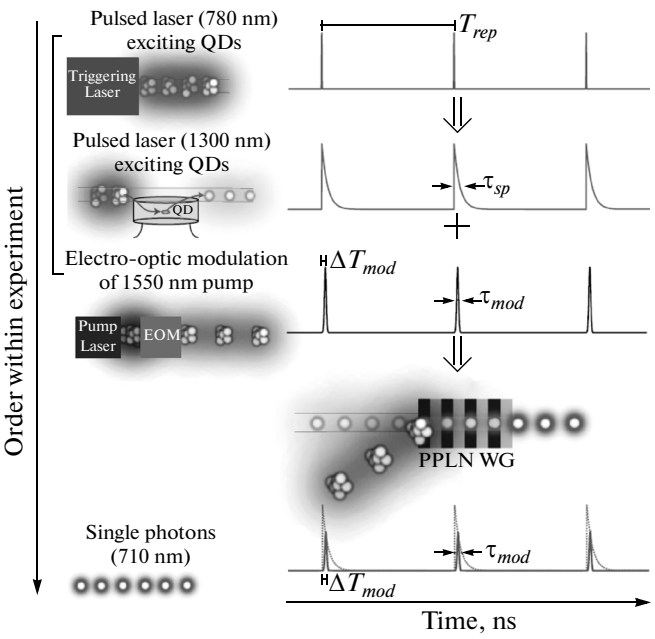

Fig. 7. Schematics of experiment on the enhancement of generation frequency of a single photon source based on QDs. T_{rep} is the repetition period of laser pulses exciting QDs, τ_{sp} is the characteristic time of photon emission from QD, ΔT_{mod} and τ_{mod} are the delay time and half width of the modulator pulse, and PPLN WG—$LiNbO_3$ is a waveguide with a one-dimensional periodic structure [32].

of $W = 0.72$ for two photons emitted from the single InAs QD at the Purcell factor $F = 28$.

The two-level system is used in the majority of the experimental studies on single photon generation in the QDs. It is possible to increase the degree of indistinguishability between the two photons emitted from the QDs when the three-level system, which is less sensitive to the excited state dephasing under condition of large detuning, is used [29]. The generation of highly indistinguishable single photons emitted from the QDs in the process of the electron spin inversion described by the three-level system via the laser excitation of the QDs into the trion state is presented in [36]. The experiment was conducted at 4.2 K in the presence of a magnetic field applied to the planar MC structure containing the AlGaAs QD ensemble in the Feucht geometry (see detailed information on the methods for the spin state control of the singly charged QDs in the external magnetic field in section 3 of this review). The energy level diagram of the QDs in the magnetic field is presented in Fig. 8a. The pulsed laser and two continuous lasers were used for excitation of the single QD. The laser frequency δ detuning from the frequency of the respective QD transitions from the spin states to the trion ones was sufficiently large to ensure that the trion states were virtually populated (Raman regime). The value of the autocorrelation function $g_{\parallel}^{(2)}(0) = 0.01$ measured with the help of the

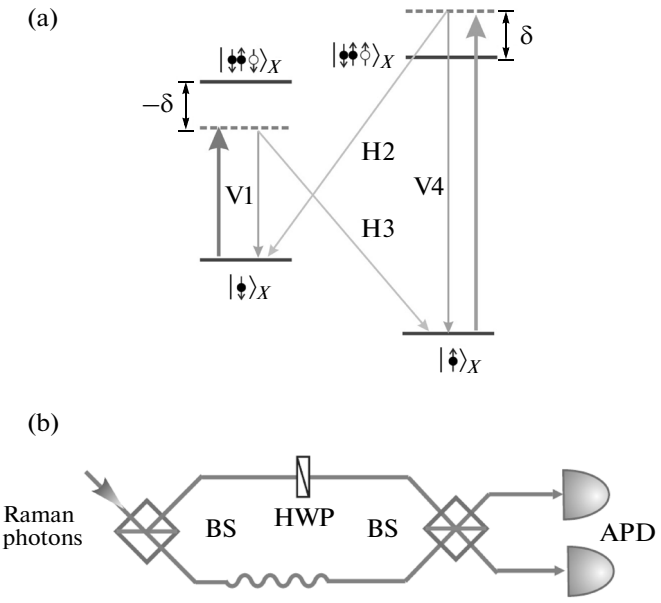

Fig. 8. Diagram of spin and trion levels of semiconductor QDs in a constant magnetic field under condition of Feucht geometry: (a) according to the selection rules photon absorption with vertical (V) (horizontal, H) polarization initiates direct (slanted) transitions from the spin states $|\uparrow\rangle_X$, $|\downarrow\rangle_X$ to trion states $|\downarrow\uparrow\Downarrow\rangle_X$, $|\downarrow\uparrow\Uparrow\rangle_X$. Interference measurement principle of two emitted Raman photons (b) under continuous QD excitation. The photon beam is split by beam splitter BS into two beams, one of which is delayed by the optic fiber for 10 ns, and the second one is transmitted through a rotating half-wave plate (HWP) determining photon polarization. The photon detection conducted by two avalanche photodiodes, APD [36].

Mach–Zehnder interferometer (Fig. 8b) for the two interfering photons with the same polarization in the case of the continuous excitation of the single QD at the detuning $\delta = 2.5$ GHz indicates the high degree of their indistinguishability. The measurement of the autocorrelation function $g_{\perp}^{(2)}(0)$ for the two photons with orthogonal polarization gives the value of 0.5 indicating their distinguishability. Interference of the two single photons emitted from the QDs was characterized by the value $u = 1 - g_{\parallel}^{(2)}(0)/g_{\perp}^{(2)}(0)$, which was 0.98 in this case. The high degree of indistinguishability was also obtained on the pulsed pumping, although their interference decreased slightly ($u = 0.95$). It is necessary to know how to generate indistinguishable photons from the separated quantum sources in order to design the photon quantum network. The authors in [36] were able to demonstrate the generation of indistinguishable photons from the two *separated* QDs located at a distance of 1.5 m in different samples with a high maximum value of the parameter $u = 0.87$.

Hence, it can be seen that the single photon sources based on the hybrid QD + MC systems are highly efficient and are accompanied by a high degree of indistinguishability of the emitted photons. It is mainly related to the fact that the MCs increase the rate of the spontaneous emission of the QDs, which is in resonance with it. Moreover, the generation of indistinguishable photons from the separated QD-sources opens additional possibilities for the design of solid-state quantum photonic networks.

ACKNOWLEDGMENTS

This study was supported by the Russian Foundation for Basic Research, project no. 13-07-00711.

REFERENCES

1. Tsukanov, A.V. and Kateev, I.Yu., Quantum calculations on quantum dots in semiconductor microcavities. Part I, *Russ. Microelectron.*, 2014, vol. 43, no. 5, pp. 315–327.
2. Hennessy, K., Badolato, A., Winger, M., Gerace, D., Atature, M., Gulde, S., Fält, S., Hu, E., and Imamoğlu, A., Quantum nature of a strongly coupled single quantum dot–cavity system, *Nature*, 2007, vol. 445, p. 896.
3. Luxmoore, I.J., Ahmadi, E.D., Wasley, N.A., Fox, A.M., Tartakovskii, A.I., Krysa, A.B., and Skolnick, M.S., Control of spontaneous emission from InP single quantum dots in GaInP photonic crystal nanocavities, *Appl. Phys. Lett.*, 2010, vol. 97, p. 181104.
4. Hoang, T.B., Beetz, J., Midolo, L., Skacel, M., Lermer, M., Kamp, M., Höfling, S., Balet, L., Chauvin, N., and Fiore, A., Enhanced spontaneous emission from quantum dots in short photonic crystal waveguides, *Appl. Phys. Lett.*, 2012, vol. 100, p. 061122.
5. Winger, M., Badolato, A., Hennessy, K.J., Hu, E.L., and Imamoğlu, A., Quantum dot spectroscopy using cavity quantum electrodynamics, *Phys. Rev. Lett.*, 2008, vol. 101, p. 226808.
6. Englund, D., Majumdar, A., Faraon, A., Toishi, M., Stoltz, N., Petroff, P., and Vučković, J., Resonant excitation of a quantum dot strongly coupled to a photonic crystal nanocavity, *Phys. Rev. Lett.*, 2010, vol. 104, p. 073904.
7. Englund, D., Faraon, A., Fushman, I., Stoltz, N., Petroff, P., and Vučković, J., Controlling cavity reflectivity with a single quantum dot, *Nature*, 2007, vol. 450, p. 857.
8. Majumdar, A., Papageorge, A., Kim, E.D., Bajcsy, M., Kim, H., Petroff, P., and Vučković, J., Probing of single quantum dot dressed states via an off-resonant cavity, *Phys. Rev. B*, 2011, vol. 84, p. 085310.
9. Stumpf, W.S., Asano, T., Kojima, T., Fujita, M., Tanaka, Y., and Noda, S., Reflectance measurement of two-dimensional photonic crystal nanocavities with embedded quantum dots, *Phys. Rev. B*, 2010, vol. 82, p. 075119.
10. Kim, E.D., Majumdar, A., Kim, H., Petroff, P., and Vučković, J., Differential reflection spectroscopy of a single quantum dot strongly couples to a photonic crystal cavity, *Appl. Phys. Lett.*, 2010, vol. 97, p. 053111.
11. Faraon, A., Fushman, I., Englund, D., Stoltz, N., Petroff, P., and Vuckovic, J., Dipole induced transpar-

ency in waveguide coupled photonic crystal cavities, *Opt. Express*, 2008, vol. 16, p. 12154.

12. Skacel, M., Pagliano, F., Hoang, T., Midolo, L., Fattahpoor, S., Li, L., Linfield, E.H., and Fiore, A., Coupling of single quantum dots to photonic crystal cavities investigated by low-temperature scanning near-field microscopy, *Phys. Rev. B*, 2013, vol. 88, p. 035416.
13. Hofbauer, F., Grimminger, S., Angele, J., Böhm, G., Meyer, R., Amann, M.C., and Finley J.J., Electrically probing photonic bandgap phenomena in contacted defect nanocavities, *Appl. Phys. Lett.*, 2007, vol. 91, p. 201111.
14. Madsen, K.H., and Lodahl, P., Quantitative analysis of quantum dot dynamics and emission spectra in cavity quantum electrodynamics, *New J. Phys.*, 2013, vol. 15, p. 025013.
15. Faraon, A., Fushman, I., Englund, D., Stoltz, N., Petroff, P., and Vučković, J., Coherent generation of non-classical light on a chip via photon-induced tunneling and blockade, *Nat. Phys.*, 2008, vol. 4, p. 859.
16. Reinhard, A., Volz, T., Winger, M., Badolato, A., Hennessy, K.J., Hu, E.I., and Imamoğlu, A., Strongly correlated photons on a chip, *Nat. Photonics*, 2012, vol. 6, p. 93.
17. Thyrrestrup, H., Sapienza, and L., Lodahl, P., Extraction of the β-factor for single quantum dots couples to a photonic crystal waveguide, *Appl. Phys. Lett.*, 2010, vol. 96, p. 231106.
18. Englund, D., Fattal, D., Waks, E., Solomon, G., Zhang, B., Nakaoka, T., Arakawa, Ya., Yamamoto, Yo., and Vučković, J., Controlling the spontaneous emission rate of single quantum dots in a two-dimensional photonic crystal, *Phys. Rev. Lett.*, 2005, vol. 95, p. 013904.
19. Gallardo, E., Martínez, L.J., Nowak, A.K., van der Meulen, H.P., Calleja, J.M., Tejedor, C., Prieto, I., Granados, D., Taboada, A.G., García, J.M., and Postigo, P.A., Emission polarization control in semiconductor quantum dots couples to a photonic crystal microcavity, *Opt. Express*, 2010, vol. 18, p. 13301.
20. Nakamura, T., Asano, T., Kojima, K., Kojima, T., and Noda, S., Controlling the emission of quantum dots embedded in photonic crystal nanocavity by manipulating Q-factor and detuning, *Phys. Rev. B*, 2011, vol. 84, p. 245309.
21. Nomura, M., Iwamoto, S., Nakaoka, T., Ishida, S., and Arakawa, Ya., Localized excitation of InGaAs quantum dots by utilizing a photonic crystal nanocavity, *Appl. Phys. Lett.*, 2006, vol. 88, p. 141108.
22. Akahane, Y., Asano, T., Song, B.-S., and Noda, S., High-Q photonic nanocavity in a two-dimensional photonic crystal, *Nature*, 2003, vol. 425, p. 944.
23. Ota, Y., Shirane, M., Nomura, M., Kumagai, N., Ishida, S., Iwamoto, S., Yorozu, S., and Arakawa, Y., Vacuum Rabi splitting with a single quantum dot embedded in a H1 photonic crystal nanocavity, *Appl. Phys. Lett.*, 2009, vol. 94, p. 033102.
24. Laucht, A., Hofbauer, F., Hauke, N., Angele, J., Stobbe, S., Kaniber, M., Böhm, G., Lodahl, P., Amann, M.-C., and Finley, J.J., Electrical control of spontaneous emission and strong coupling for a single quantum dot, *New J. Phys.*, 2009, vol. 11, p. 023034.
25. Brossard, F.S.F., Xu, X.L., Williams, D.A., Hadjipanayi, M., Hugues, M., Hopkinson, M., Wang, X., and Taylor, R.A., Strongly couples single quantum dot in a photonic crystal waveguide cavity, *Appl. Phys. Lett.*, 2010, vol. 97, p. 111101.
26. Kok, P., Nemoto, K., Ralph, T.C., Dowling, J.P., and Milburn, G.J., Linear optical quantum computing with photonic qubits, *Rev. Mod. Phys.*, 2007, vol. 79, p. 135.
27. O'Brien, J.L., Furusawa, A., and Vuckovic, J., Photonic quantum technologies, *Nat. Photonics*, 2009, vol. 23, p. 687.
28. Pan, J.-W., Chen, Z.-B., Lu, C.-Y., Weinfurter, H., Zeilinger, A., and Zukowski, M., Multiphoton entanglement and interferometry, *Rev. Mod. Phys.*, 2012, vol. 84, p. 777.
29. Kiraz, A., Atatüre, M., and Imamoğlu, A., Quantum-dot single-photon sources: prospects for applications in linear optics quantum information processing, *Appl. Phys. Lett.*, 2004, vol. 69, p. 032305.
30. Stace, T.M., Milburn, G.J., and Barnes, C.H.W., Entangled two-photon source using biexciton emission of an asymmetric quantum dot in a cavity, *Phys. Rev. B*, 2003, vol. 67, p. 085317.
31. Schwagmann, A., Kalliakos, S., Farrer, I., Griffiths, J.P., Jones, G.A.C., Ritchie, D.A., and Shields, A.J., On-chip single photon emission from an integrated semiconductor quantum dot into a photonic crystal waveguide, *Appl. Phys. Lett.*, 2011, vol. 99, p. 261108.
32. Rakher, M.T., Ma, L., Davanço, M., Slattery, O., Tang, X., and Srinivasan, K., Simultaneous wavelength translation and amplitude modulation of single photons from a quantum dot, *Phys. Rev. Lett.*, 2011, vol. 107, p. 083602.
33. Kaniber, M., Neumann, A., Laucht, A., Huck, M.F., Bichler, M., Amann, M.-C., and Finley, J.J., Efficient and selective cavity-resonant excitation for single photon generation, *New J. Phys.*, 2009, vol. 11, p. 013031.
34. Laurent, S., Varoutsis, S., Le Gratiet, L., Lemaître, A., Sagnes, I., Raineri, F., Levenson, A., Robert-Philip, I., and Abram, I., Indistinguishable single photons from a single quantum dot in a two-dimensional photonic crystal cavity, *Appl. Phys. Lett.*, 2005, vol. 87, p. 163107.
35. Bylander, J., Robert-Philip, I., and Abram, I., Interference and correlation of two independent photons, *Eur. Phys. J. D*, 2003, vol. 22, p. 295.
36. He, Y., He, Y.-M., Wei, Y.-J., Jiang, X., Chen, M.-C., Xiong, F.-L., Zhao, Y., Schneider, C., Kamp, M., Höfling, S., Lu, C.-Y., and Pan J.-W., Indistinguishable tunable single photons emitted by spin-flip Raman transitions in InGaAs quantum dots, *Phys. Rev. Lett.*, 2013, vol. 111, p. 237403.

Translated by L. Brovko